Title

Photoreceptor Cell Calcium Dysregulation and Calpain Activation Promote Pathogenic Photoreceptor Oxidative Stress and Inflammation in Prodromal Diabetic Retinopathy.

Journal

The American journal of pathology, 191(10)

ISSN

0002-9440

Authors

Saadane, Aicha
Du, Yunpeng
Thoreson, Wallace B
et al.

Publication Date

2021-10-01

DOI

10.1016/j.ajpath.2021.06.006

The American Journal of Pathology, Vol. 191, No. 10, October 2021

The American Journal of
PATHOLOGY
ajp.amjpathol.org

METABOLIC, ENDOCRINE, AND GENITOURINARY PATHOBIOLOGY

Photoreceptor Cell Calcium Dysregulation and Calpain Activation Promote Pathogenic Photoreceptor Oxidative Stress and Inflammation in Prodromal Diabetic Retinopathy

Aicha Saadane,* Yunpeng Du,* Wallace B. Thoreson,[†‡] Masaru Miyagi,[§] Emma M. Lessieur,* Jianying Kiser,* Xiangyi Wen,[†] Bruce A. Berkowitz,[¶] and Timothy S. Kern*[‖]

From the Department of Ophthalmology, University of California, Irvine, Irvine, California; the Departments of Ophthalmology and Visual Sciences,[†] and the Pharmacology and Experimental Neuroscience,[‡] University of Nebraska Medical Center, Omaha, Nebraska; the Department of Pharmacology,[§] Case Western Reserve University, Cleveland, Ohio; the Department of Ophthalmology,[¶] Visual and Anatomical Sciences, Wayne State University School of Medicine, Detroit, Michigan; and the Veterans Administration Medical Center Research Service,[‖] Long Beach, California

Accepted for publication June 15, 2021.

Address correspondence to Aicha Saadane, Ph.D., Department of Ophthalmology, University of California, Irvine, 837 Health Sciences Rd., Gillespie Neuroscience Bldg. Room 2107, Irvine, CA 92697-4375. E-mail: asaadane@hs.uci.edu.

This study tested the hypothesis that diabetes promotes a greater than normal cytosolic calcium level in rod cells that activates a Ca^{2+}-sensitive protease, calpain, resulting in oxidative stress and inflammation, two pathogenic factors of early diabetic retinopathy. Nondiabetic and 2-month diabetic C57Bl/6J and calpain1 knockout (*Capn1*$^{-/-}$) mice were studied; subgroups were treated with a calpain inhibitor (CI). Ca^{2+} content was measured in photoreceptors using Fura-2. Retinal calpain expression was studied by quantitative RT-PCR and immunohistochemistry. Superoxide and expression of inflammatory proteins were measured using published methods. Proteomic analysis was conducted on photoreceptors isolated from untreated diabetic mice or treated daily with CI for 2 months. Cytosolic Ca^{2+} content was increased twofold in photoreceptors of diabetic mice as compared with nondiabetic mice. Capn1 expression increased fivefold in photoreceptor outer segments of diabetic mice. Pharmacologic inhibition or genetic deletion of *Capn1* significantly suppressed diabetes-induced oxidative stress and expression of proinflammatory proteins in retina. Proteomics identified a protein (WW domain-containing oxidoreductase [WWOX]) whose expression was significantly increased in photoreceptors from mice diabetic for 2 months and was inhibited with CI. Knockdown of *Wwox* using specific siRNA *in vitro* inhibited increase in superoxide caused by the high glucose. These results suggest that reducing Ca^{2+} accumulation, suppressing calpain activation, and/or reducing Wwox up-regulation are novel targets for treating early diabetic retinopathy. *(Am J Pathol 2021, 191: 1805–1821; https://doi.org/10.1016/j.ajpath.2021.06.006)*

The pathogenesis of diabetic retinopathy (DR), a leading cause of vision loss and blindness, is not fully understood, and therefore effective treatment options remain limited. In experimental models, diabetes-induced degeneration of retinal capillaries and other lesions of the retina have been inhibited by antioxidant or anti-inflammatory strategies, suggesting that oxidative stress and inflammation play an important role in the early development of the retinopathy. Recent studies provide evidence that photoreceptor cells, the most numerous cell type in the retina, play a causal role in the microvascular disease of DR[1–3] and are a major source of reactive oxygen species (ROS) and inflammatory proteins

Supported by NIH grants EY022938 and R24 EY024864 (T.S.K.), R01EY026584 and R01AG058171 (B.A.B.), and EY010542 (W.B.T.); a Senior Scientific Investigator Award from Research to Prevent Blindness (W.B.T.); the Department of Veterans Affairs grant BX003604 (T.S.K.); NEI Core grants P30 EY04068 and P30EY11373 (B.A.B.); and unrestricted grants from Research to Prevent Blindness (Kresge Eye Institute), and Department of Ophthalmology University of California, Irvine.

Disclosures: None declared.

https://doi.org/10.1016/j.ajpath.2021.06.006

and cytokines in diabetes.[4–7] Factors involved in promoting photoreceptor oxidative stress and inflammation during prodromal DR remain unclear.

Maintaining Ca^{2+} homeostasis is vital for cell health and is tightly regulated.[8] *In vivo* imaging studies using manganese-enhanced magnetic resonance imaging have shown that influx of Ca^{2+} and other ions in retinal cells (especially photoreceptors) is disrupted early in the course of diabetes. This defect can be corrected by a variety of antioxidant treatments, showing that oxidative stress and calcium dysregulation are interconnected.[4,9–11] It remains unclear whether abnormal calcium handling in diabetes can also promote oxidative stress, the focus of this study.

One important consequence of Ca^{2+} dysregulation is activation of Ca^{2+}-dependent proteases in the calpain family. Calpains are responsible for limited proteolysis of target proteins, potentially leading to the activation or inhibition of enzymes and kinases. Excessive calpain activation has been implicated in the development of complications in a variety of tissues, including complications of diabetes, at least in the heart and brain.[12–17] Calpains regulate the pathogenic mitochondrial oxidative stress in diabetic cardiomyopathy, which can be inhibited by overexpression of mitochondrial calpastatin, an endogenous calpain inhibitor (CI).[18] Because photoreceptor cells in the retina are the major site of retinal superoxide generation in diabetes,[7] and contain approximately 75% of the retina's mitochondria, we postulated that calpains might play a role in diabetes-induced photoreceptors oxidative stress and induction of proinflammatory proteins in the retina in diabetes.

This study addresses the above knowledge gaps by measuring i) Ca^{2+} levels from rod photoreceptor cells in retinal slices of diabetic mice, ii) calpain expression and activity in retinas of diabetic mice, iii) the impact of *in vivo* administration of a CI or genetic deletion of *Capn1* on diabetes-induced oxidative stress and expression of inflammatory proteins in the retina, and iv) diabetes-induced abnormalities of the photoreceptor proteome that are influenced by calpain activity. Finally, this study identified Wwox as a novel substrate of calpain that contributes to the hyperglycemia-induced generation of superoxide by the retina.

Materials and Methods

This study was performed in strict accordance with the NIH's *Guide for the Care and Use of Laboratory Animals*,[19] the Association for Research in Vision and Ophthalmology (ARVO) Statement for the Use of Animals in Ophthalmic and Vision Research,[20] and with authorization of the institutional animal and care use committees at Case Western Reserve University, University of California, Irvine, Wayne State University, and the University of Nebraska Medical Center. All efforts were made to minimize suffering within the context of the diabetic protocol including administration of insulin to prevent weight loss.

Mice

Wild-type (WT) C57Bl/6J mice were obtained from the Jackson Laboratory (Bar Harbor, ME). Calpain1 knockout ($Capn1^{-/-}$) mice (C57Bl/6j background) were obtained from the laboratory of Dr. Chishti (Tufts University School of Medicine, Boston, MA).[21] In all studies, male mice (2-month−old) were randomly assigned to become diabetic or remain as nondiabetic controls. Diabetes was induced by five sequential daily intraperitoneal injections of a freshly prepared solution of streptozotocin in citrate buffer (pH 4.5) at 55 to 60 mg/kg of body weight. Hyperglycemia was verified at least three times during the second week after streptozotocin administration, and mice having three consecutive measurements of fasting blood glucose >275 mg/dL were classified as being diabetic. Insulin was given as needed to prevent weight loss without preventing hyperglycemia and glucosuria (0 to 0.2 U of NPH insulin subcutaneously 0 to 3 times per week). All animals were maintained on a standard 12-hour light (~10 lux)-dark cycle and were provided standard rodent chow (Purina TestDiet 5001; Purina, Richmond, IN) and water *ad libitum*. Blood glucose and hemoglobin A1c were measured as reported previously.[7,22] Body weight was measured weekly. Once declared diabetic, some mice received a daily intraperitoneal injection (10 mg/kg body weight) of CI (carbobenzoxy-valinyl-phenylalaninal, also known as MDL 28170; Calbiochem, Burlington, MA) dissolved in dimethyl sulfoxide. At 2 months of diabetes (4 months of age), retinal structure and function were characterized, and then animals were euthanized and eyes collected.

Regarding the measurement of calcium in retinal photoreceptor cells, the experiments were done between 10 AM and 2 PM during circadian day, and the tissue was light adapted (because of the bright 340/380-nm fluorescence used to measure calcium changes, the eyes were not dissected in the dark). For calpain activity and calpain1 immunohistochemistry studies, mice were in the normal light cycle, and the eyes were collected before 1:30 PM.

Retinal Imaging and Visual Function

The authors conducted an anatomic characterization of $Capn1^{-/-}$ and WT mice using spectral domain-optical coherence tomography (OCT; the 840 HHP spectral domain-OCT system; Bioptigen, Durham, NC), and electroretinographic (ERG; Diagnosys Celeris rodent ERG device; Diagnosys, Lowell, MA) recordings as described,[23,24] except that for ERG analysis, mice were anesthetized using isoflurane. Retinal morphology was further confirmed by histology. After enucleation, eyes were fixed in formalin (10% neutral buffered) for 48 hours. Paraffin-embedding, sectioning, hematoxylin and eosin staining, and image

scanning were performed by the Histowiz company (Brooklyn, NY).

Fura-2 Measurements in Retinal Photoreceptor Cells

For Ca^{2+} imaging in mouse vertical retinal slices, mice were euthanized by carbon dioxide asphyxiation under dim red light. Subsequent dissections were performed under infrared illumination using GenIII night vision goggles (Nitemate NavIII; Litton Industries, Watertown, CT) mounted on a dissecting microscope. After enucleation, the eye was hemisected and the retina mounted vitreal side down on a nitrocellulose membrane (5 × 10 mm; type AAWP, 0.8-μm pores; Millipore, Billerica, MA). The retina was cut into 125-μm slices using a razor blade tissue slicer (Stoelting, Wood Dale, IL). Slices were rotated 90 degrees to view the retinal layers and anchored in the recording chamber by embedding the ends of the nitrocellulose membrane in vacuum grease so that measurement could be make from cells in the photoreceptor layer. The recording chamber was mounted on an upright fixed-stage microscope (Nikon E600FN; Nikon Instruments, Melville, NY), and slices were superfused at approximately 1 mL per minute with Ames' medium (US Biological, Salem, MA) bubbled with 95% O_2 and 5% CO_2 (35°C).

For measurements of intracellular Ca^{2+} $[Ca^{2+}]_i$, the ratiometric dye Fura-2 (Invitrogen, Carlsbad, CA) was used. Retinal slices were loaded with Fura-2 by incubating them at room temperature for 2 hours with 0.5 mL of 10 μmol/L Fura-2/AM in Hibernate-A medium (Brain Bits LLC, Springfield, IL) in darkness. An epifluorescence lamp (150 W, Xe) was attached to a Lambda 10 to 2 filter wheel (Sutter Instruments, Novato, CA), equipped with 340- and 380-nm interference filters, and coupled to the microscope (E600FN; Nikon Instruments) through a liquid light guide (Sutter Instruments). Images were acquired through a 60× (1.0 numerical aperture ; Nikon Instruments) water immersion objective using a cooled electron multiplying charge-coupled device camera (Rolera MGi Plus; QImaging, Surrey, BC, Canada) and Nikon NIS-Elements AR 4.50.0 software. $[Ca^{2+}]_i$ was determined using the formula: $[Ca^{2+}]_i = K_d (F_{min}/F_{max}) [(R\text{-}R_{min})/(R_{max}\text{-}R)]$ where $K_d = 224$ nmol/L Ca^{2+}, r = ratio of fluorescence emitted at 510 nm by excitation with 340- and 380-nm light, F_{min} = highest fluorescence emission measured with 380-nm excitation, and F_{max} = lowest 380-nm emission. The minimum 340/380 ratio (R_{min}) was determined by bath application of ionomycin (10 μmol/L) in a Ca^{2+}-free solution containing 5 mmol/L EGTA. The maximum 340/380 ratio (R_{max}) was then measured by bath application of ionomycin in control Ames' solution. Resting Ca^{2+} values in rods were measured at 5-second intervals in regions of interest placed on rod somas and averaged over the first 1 to 2 minutes of recording. Measurements were averaged from 2 to 10 rods in each slice preparation to yield a single value for each eye.

Calpain Activity

Retinal calpain activity was determined using three methods. In the first, the right eye of diabetic and nondiabetic mice was injected intravitreally with 1 μL of fluorogenic calpain substrate IV (Catalog # 208,773; Calbiochem, Burlington, MA) at 10 μmol/L under visualization from a dissecting microscope. Two hours later, mice were sacrificed, and eyes were fresh frozen in OCT medium (Tissue-Tek; Sakura, Torrance, CA) and stored at −80°C until cryosectioned. In the second method, whole eyes from nondiabetic and diabetic mice were embedded in OCT and stored at −80°C until cryosectioned. Twelve-micron thick sections were air dried for 30 minutes at room temperature, hydrated 3 × 5 minutes in phosphate-buffered saline (PBS), and incubated with fluorogenic calpain substrate at room temperature for 1 hour (Millipore Sigma, St. Louis, MO) with or without CI (10 μmol/L), then rinsed in distilled water and mounted with Prolong Gold containing DAPI (Invitrogen) for nuclear staining and viewed using an inverted fluorescence microscope. In the third method, calpain activation was monitored by the proteolysis of a calpain substrate, spectrin, using an antibody against the cleaved spectrin fragment.

Immunofluorescence

Twelve-micron retinal sections were warmed to room temperature for 30 minutes and washed three times for 5 minutes in PBS. Sections were then blocked for 1 hour with 5% normal goat serum (Invitrogen) in PBS containing 0.05% Tween 20 (blocking buffer). Sections were incubated overnight at 4°C with rabbit anti-calpain1 (A1172; ABclonal, Woburn, MA). The next day, slides were washed three times for 5 minutes in PBS containing 0.05% Tween 20 and incubated for 1 hour in the dark with Alexa Fluor 647 secondary antibody (111 to 605-144; Jackson ImmunoResearch Laboratories, West Grove, PA). Slides were washed three times for 5 minutes in PBS, then one time in distilled water, blotted dry, and then mounted with ProLong Gold anti-fade reagent with DAPI (P36935; Invitrogen, Carlsbad, CA). The calpain1 staining was imaged on a Keyence microscope (Keyence Corporation of America, Itasca, IL).

Lucigenin Assay of Superoxide

Superoxide levels were measured chemically with lucigenin (bis-*N*-methylacridinium nitrate), as reported previously.[25] Briefly, freshly isolated retinas were preincubated in 200 μL of Krebs-HEPES buffer (pH 7.2) with 5 or 30 mmol/L glucose for 10 minutes at 37°C in 5% CO_2. Luminescence indicating the presence of superoxide was measured 5 minutes after addition of lucigenin (5 mmol/L). Luminescence intensity is reported in arbitrary units per milligram of protein. Superoxide levels in 661W cells were measured similar to retinal samples, except about 200,000 cells were

used, and luminescence intensity is reported in arbitrary units/10^6 cells.

Vibratome Isolation of Photoreceptor Cells from Mice

A vibratome was used to bisect fresh unfixed retina into outer and inner retinas as previously described.[26] The retinas were freshly isolated, and a flat mount of the retina with appropriate radial cuts was laid flat (photoreceptor side up) on a 4% gelatin block, and 20% warm gelatin was used to cover and seal the entire retina. Cold Dulbecco's modified Eagle's medium was placed in the vibratome chamber containing the retinas. Based on the measured thickness of the photoreceptor layer of mouse retina,[26] a conservative estimate of a 40-μm thick slice was used to enrich the photoreceptor layer from the remaining retina using a Leica VT1000 S vibratome. The isolated section of photoreceptor cells was immediately placed in liquid nitrogen and stored at −80°C. Elapsed time from eye enucleation to freezing the photoreceptor layer in an Eppendorf tube was about 15 to 25 minutes.

Western Blot Analysis

One retina from each mouse was sonicated in 70 μL of lysis buffer (50 mmol/L Tris, pH 8.0, 150 mmol/L NaCl, 5 mmol/L EDTA, 1% Nonidet P-40, 0.1% SDS, and complete EDTA-free protease inhibitor mixture from Roche (Lakwood, CA). Retinal homogenates were incubated on ice for 30 minutes followed by centrifugation at 12,000 × *g* for 15 minutes at 4°C. Supernatants were used for SDS-PAGE (50 μg of protein/lane) followed by Western blot analysis, which was performed as described.[27] Proteins were visualized with the following primary antibodies: 1:200 for intercellular adhesion molecule 1 (ICAM-1; sc-71292; Santa Cruz Biotechnology, Santa Cruz, CA), 1:200 for inducible nitric oxide synthase (iNOS; 610,328; BD Biosciences, San Jose, CA), 1:100 for pIκBα (2859; Cell Signaling Technology, Danvers, MA), 1:1000 inhibitor of κBα (IκBα; 9242; Cell Signaling), and 1:1000 for cleaved spectrin (ABN2264; EMD Millipore, Temecula, CA). The secondary antibody was goat anti-rabbit IRDye 800CW (925 to 32,211; Li-Cor, Lincoln, NE; dilution 1:5000). Membranes were also incubated with primary antibody against β-actin (1:5000), which was used as a loading control (ab8226; Abcam, Cambridge, MA), and secondary goat anti-mouse IRDye 680RD (925 to 68,070; Li-Cor; dilution 1:5000). Membranes were imaged using the Odyssey infrared imaging system (Li-Cor). The densitometry results of Western blots were expressed as means ± SD.

qRT-PCR

Both retinas from each mouse were combined (total of three to four mice per group), and total RNA was isolated with TRIzol Reagent (Life Technologies, Grand Island, NY). Total RNA (1 μg) was converted to cDNA by SuperScript III Reverse Transcriptase (Invitrogen) and used for quantitative RT-PCR (qRT-PCR) conducted on a LightCycler 480 instrument (Roche). The sequences of the primers for gene quantifications were taken from qPrimerDepot, a primer database for qRT-PCR.[28] *GAPDH* was used as a housekeeping gene (Ct number approximately 14) over β-actin (Ct number ∼ 28). PCR reactions were performed in triplicate and normalized to *GAPDH*.

Cell Culture

The authors used a cone photoreceptor cell line, 661W, which they had previously confirmed by positive identification of cone opsin mRNA.[29] 661W cells were cultured in Dulbecco's modified Eagle's medium containing 10% fetal bovine serum and 5 mmol/L (normal glucose) or 30 mmol/L glucose (high glucose) in 6-well plates for 5 days (the medium was changed every other day). In a different set of experiments, 661W cells were incubated with 5 mmol/L, 25 mmol/L, or 30 mmol/L glucose or equivalent concentration of D-mannitol (osmotic control), to determine the conditions that lead to the highest superoxide levels and to ascertain that the measured superoxide level is due to elevated glucose as opposed to hyperosmolar conditions.

Proteomics

Sample Preparation

Retinas were isolated from nondiabetic, diabetic, diabetic treated daily with CI (n = 3 to 4) for 2 months or their nondiabetic age-matched controls (total age 4 months) under carbon dioxide anesthesia, and stored briefly in PBS. The photoreceptor-enriched block (outer retina) was isolated from the rest of the retina using a vibratome as described above.

Protein Fractionation and In-Gel Protein Digestion

Proteins from each photoreceptor-enriched block were extracted with SDS-sample buffer, 50 μg of which was separated by SDS-PAGE. The gel was stained by Coomassie R-250, and each sample (lane) was cut into 12 segments. The proteins in each segment were in-gel digested using trypsin,[30] and the digests were analyzed by liquid chromatography with tandem mass spectrometry (MS/MS) as described below.

Liquid Chromatography with MS/MS Analysis

Liquid chromatography with MS/MS analysis was performed using a Finnigan LTQ-Orbitrap Elite hybrid mass spectrometer system (Thermo Scientific, Bremen, Germany). The tryptic digests were chromatographed on a reversed-phase 0.075 × 150-mm C18 Acclaim PepMap 100 column (Dionex Inc., Sunnyvale, CA) using a linear gradient of acetonitrile from 2% to 40% over 5 to 110 minutes in aqueous 0.1% formic acid at a flow rate of 300 nL per minute. The eluent was directly introduced into the mass spectrometer operated

Table 1 Metabolic Control in WT and *Capn1*$^{-/-}$, Nondiabetic, Diabetic, and Diabetic Mice Treated with Calpain Inhibitor

Group	*n*	Final bw, g	Blood glucose, fasting, mg/dL	HbA1c, %
WT N	10	38 ± 3.9	130 ± 21	2.9 ± 0.1
WT D	16	29 ± 2.3	489 ± 70	8 ± 0.3
WT D + calpain inhibitor	5	27 ± 2.5	448 ± 94	7.6 ± 0.9
Capn1$^{-/-}$ N	9	30 ± 2.9	145 ± 22.8	
Capn1$^{-/-}$ D	8	23 ± 2.7	443 ± 115.9	
WT N	10	30 ± 1.8	160 ± 45.6	
WT D	10	26 ± 2.9	494 ± 65.36	

Data are expressed as means ± SD.
bw, body weight; D, diabetic; HbA1c, hemoglobin A1c; N, nondiabetic; WT, wild type.

in a data-dependent MS to MS/MS switching mode, with the 15 most intense ions in each MS scan subjected to MS/MS analysis. The full MS scan was performed at a resolution of 60,000 in the Orbitrap detector, and the MS/MS scans were performed in the ion trap detector in collision-induced dissociation mode. The fragmentation was performed using the collision-induced dissociation mode with a normalized collision energy of 35 eV.

Database Searching and Label-Free Quantification

RAW MS files were imported to MaxQuant software version 1.5.2.8 (Max-Planck-Institute of Biochemistry, Planegg, Germany)[31] with Andromeda as the search engine for protein identification and label-free quantitation (LFQ).[32] The protein samples from the three experimental groups were analyzed as one set. Proteins were identified by comparing all the experimental peptide MS/MS spectra against the UniProt mouse canonical database (UniProt, *https://www.uniprot.org*, last accessed July 2017). Carbamidomethylation of cysteine was set as a fixed modification, whereas oxidation of methionine to methionine sulfoxide and acetylation of N-terminal amino group were set to be variable modifications. LFQ was enabled, and the LFQ minimum ratio count was set to 1. Remaining options were kept as default.

Proteomic Data and Statistical Analysis

The output file, ProteinGroups.txt, from the MaxQuant database search was imported to Perseus software version 1.6.0.7 (Max-Planck-Institute of Biochemistry)[33] to compare protein expression between the three sample groups. MaxQuant-derived LFQ protein intensities were log2 transformed before further analysis. Data imputation for missing values was then done by a normal distribution

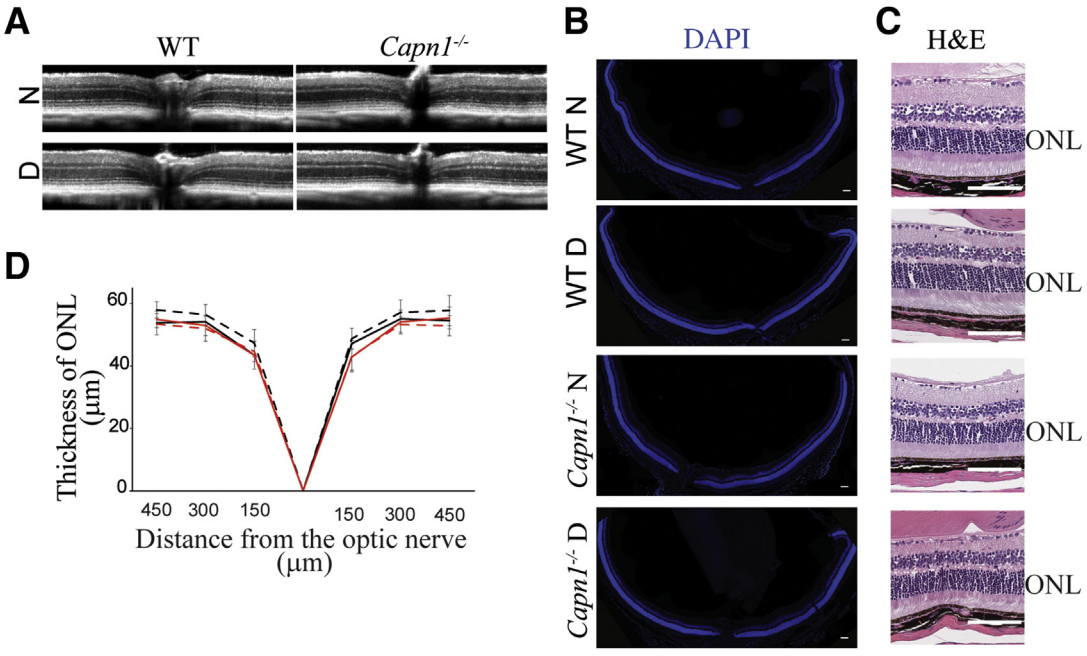

Figure 1 Retinal thickness is not affected by *Capn1* deletion or diabetes. **A** and **D:** Spectral domain-optical coherence tomography images (**A**) and quantification of data (**D**) show that the deletion of *Capn1* (**solid red lines**) alone or in conjunction with diabetes (**dashed red lines**) resulted in essentially no loss of retinal photoreceptors (ONL thickness) compared with nondiabetic (**solid black lines**) or diabetic (**dashed black lines**) mice. **B** and **C:** Histologic images of the entire retina (horizontal temporal-nasal orientation) stained with DAPI (**B**) or hematoxylin and eosin (H&E) (**C**) confirm a normal organization of the retinas in all four groups of mice. Data are expressed as means ± SD. $n = 8$ mice (16 retinas) per group (**D**). Scale bars: 100 μm. D, 2 months diabetic; N, nondiabetic; ONL, outer nuclear layer; WT, wild type.

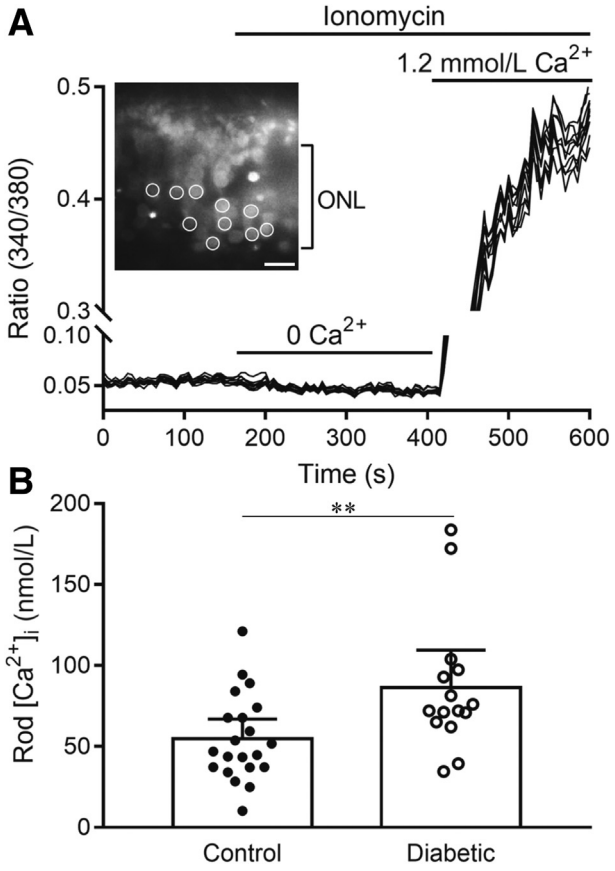

Figure 2 Resting intracellular Ca^{2+} levels are elevated significantly in rod cells from diabetic mice. **A:** Illustration of the measurement protocol. The **inset** shows a section of retina from a control mouse labeled with Fura2 and excited by 380 nm light. In this example, measurements were made from regions of interest positioned on 10 rod somas (**circles**). After measuring basal Ca^{2+} levels for 2 minutes, ionomycin (10 mmol/L) was applied with a Ca^{2+}-free solution to measure the minimum 340/380 ratio (Rmin). Ca^{2+} was then elevated to approximately 1.2 mmol/L by applying Ames' medium in the presence of ionomycin to measure Rmax. **B:** Average basal Ca^{2+} levels were measured. The individual data points represent average measurements made from 2 to 10 rods in each eye [$n = 21$ control eyes (12 mice), 15 diabetic eyes (10 mice)]. The two samples showed a statistically significant difference. Data are expressed as means with 95% CIs. $n = 21$ control eyes (from 12 mice) and 15 diabetic eyes (from 10 mice) (**B**). $^{**}P \leq 0.01$. ONL, outer nuclear layer.

method.[33] Each datum was normalized by subtracting a median value of the data. Two-sample *t*-test (two-tailed distribution and two-sample equal variance) was used to estimate the significance levels for the difference in protein expressions between the nondiabetic versus diabetic and diabetic versus diabetic treated mice using RStudio software version 3.3.2 (RStudio, Boston, MA; *http://www.rstudio.com*). $P < 0.05$ was considered significant.

WWOX Knockdown Using siRNA

In order to knock down *Wwox in vitro*, siRNA against mouse WW domain-containing oxidoreductase (WWOX), and control scrambled siRNA obtained from Ambion (Life Technology, Carlsbad, CA) were used. Transfection was performed using Lipofectamine RNAiMAX Reagent (Invitrogen) according to the manufacturer's protocol. Briefly, these were mixed in separate tubes with Lipofectamine RNAiMAX Reagent with opti-MEM medium without serum, and diluted siRNA with opti-MEM medium without serum. The siRNA concentrations of 5 pmol/L and 25 pmol/L were selected based on a preliminary dose-response experiment. The diluted siRNAs were added to the diluted Lipofectamine RNAiMAX Reagent (1:1 ratio), then incubated for 5 minutes at room temperature. siRNA–lipid complex was added to a 6-well plate, and cells were incubated at 37°C. Twenty-four hours later, the medium was discarded, and fresh culture medium containing 30 mmol/L glucose was added. The cells were then incubated for an additional 4 days before measuring superoxide using the lucigenin method as described previously.[29]

Statistical Analysis

Data are expressed as means ± SD, except for ERG measurement ($n = 10$ to 14 eyes) that are expressed as means ± SEM. Statistical analyses were performed with analysis of variance followed by Fisher's test (StatView for Windows software version 5.0.1; SAS Institute, Cary, NC), except for gene expression in diabetic versus nondiabetic retinas, which was analyzed by *t*-test, and for ERG, which was analyzed by two-way repeated-measures of variance. The mean FURA-2 and superoxide data for each eye were consistent with a normal distribution and were initially compared using two-tailed unpaired *t*-tests. However, this approach is not optimal because it requires averaging multiple measurements from a single sample and thus is not as strong an approach as taking into account correlations between each measurement from each sample. A generalized estimating equation approach performs a general linear regression analysis using contiguous locations or measurements in each subject and accounts for the within-subject correlation between contiguous locations or measurements. Thus, FURA-2 data were compared using the generalized estimating equation method.

Results

Severity of Diabetes in Animals

Clinical data from nondiabetic and diabetic WT and *Capn1*$^{-/-}$ mice are depicted in Table1. There was no significant difference with respect to glycemia between nondiabetic mice; glycemia was elevated in all diabetic mice and was not different between diabetic groups (Table 1).

Neither *Capn1* Deletion nor Diabetes Has an Effect on Retinal Thickness

The deletion of *Capn1* did not cause a significant alteration in retinal structure appearance compared with the WT retina, as

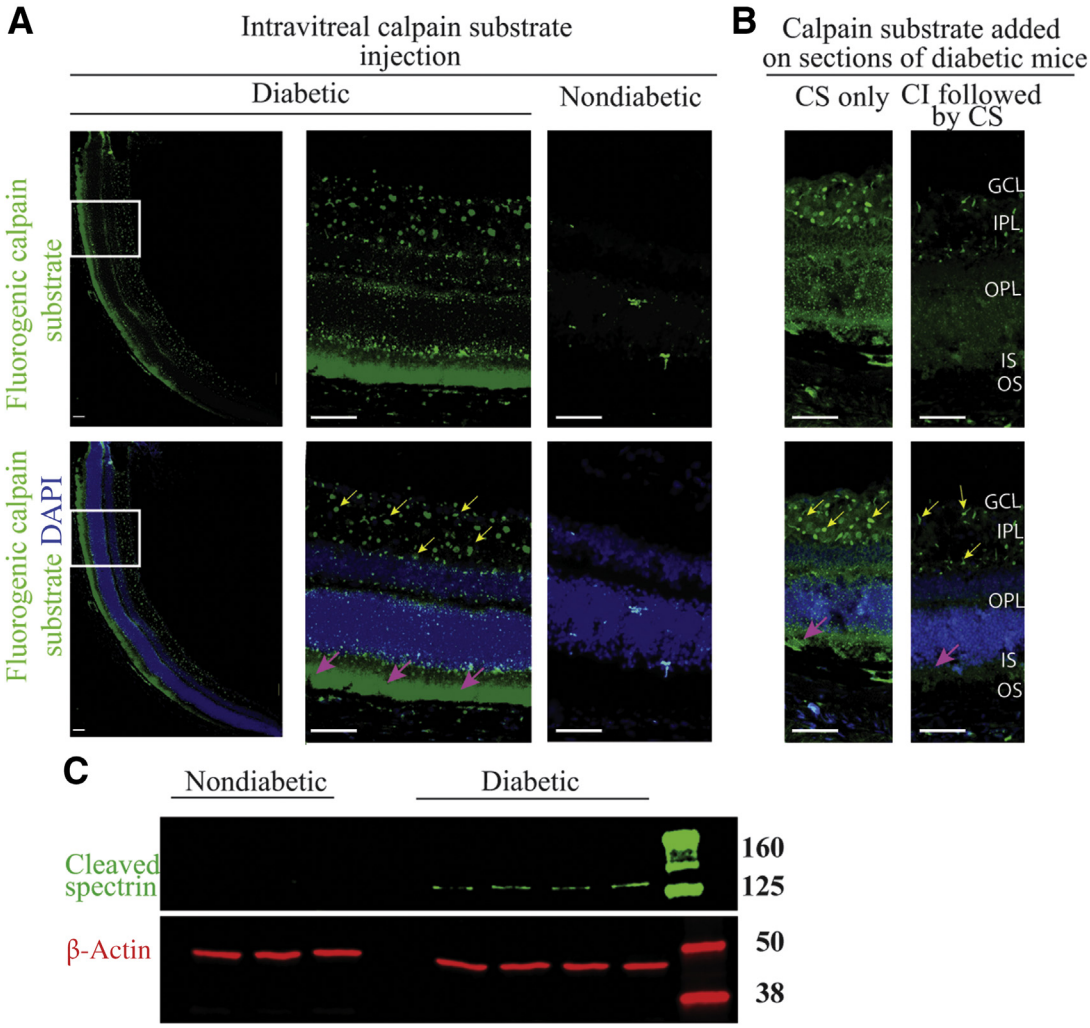

Figure 3 Calpain activity in nondiabetic and diabetic mice. **A** and **B:** Fluorogenic calpain substrate was injected intravitreally (**A**) or added on fresh-frozen cryosections (**B**) of diabetic and nondiabetic mice. In **A**, the **left panels** represent a wide view of the retina (nasal), and the **middle panels** represent enlarged view of the **boxed regions**. Calpain activity is shown with green, and nuclei were stained with DAPI (blue). Calpain activity was predominantly localized to photoreceptors of diabetic retina (**magenta arrows**) as compared with nondiabetic retina. Focal deposits of staining was present in the IPL and the GCL (**yellow arrows**). In **B**, sections were pretreated with or without calpain inhibitor (CI) before the addition of calpain substrate (CS). The pretreatment of the sections with CI abolished the staining in photoreceptors, but not of the focal staining. **C:** Calpain activity was determined by the level of cleavage of spectrin. Protein lysates were subjected to Western blotting using anti-cleaved spectrin antibody (approximately 160 kDa) and β-actin antibody (approximately 42 kDa) as loading control. Scale bars: 100 μm. GCL, ganglion cell layer; IPL, inner plexiform layer; IS, photoreceptor outer segment; OPL, outer plexiform layer; OS, photoreceptor outer segment.

indicated by OCT (Figure 1A). In addition, diabetes of 2-month duration did not cause a significant increase or decrease in retinal thickness in *Capn1*$^{-/-}$ mice (Figure 1D) when compared with WT animals. The appearance of retinal structure was further confirmed by histology. Histologic sections representing a horizontal (temporal-nasal) orientation and containing optic nerve tissue landmark showed overall normal structure (Figure 1, B and C).

Intracellular Ca^{2+} Levels Are Elevated in Photoreceptors of Diabetic Mice

Retinal photoreceptor cells have been implicated in the pathogenesis of DR, and have abnormal L-type Ca^{2+} channel (LTCC) function in diabetes.[3,7–9] Next set of experiments examined whether rod cells from dark-adapted diabetic mice (2-month duration of diabetes) exhibited greater than normal levels of intracellular Ca^{2+}. Photoreceptor cells in vertical retinal slices were loaded with the Ca^{2+}-sensitive dye Fura2, by incubation with Fura2-AM. The photoreceptor cells tested were judged to be rod cells based on their physical appearance and the greater number of rods compared with cones in the mouse retina. Basal resting intracellular calcium $[Ca^{2+}]i$ was measured in individual rod cell somas at 5-second intervals and averaged over a 2-minute period (Figure 2). Ca^{2+} sensitivity of the dye was then calibrated in each preparation by measuring R_{min} and R_{max}. As illustrated in Figure 2, R_{min} was

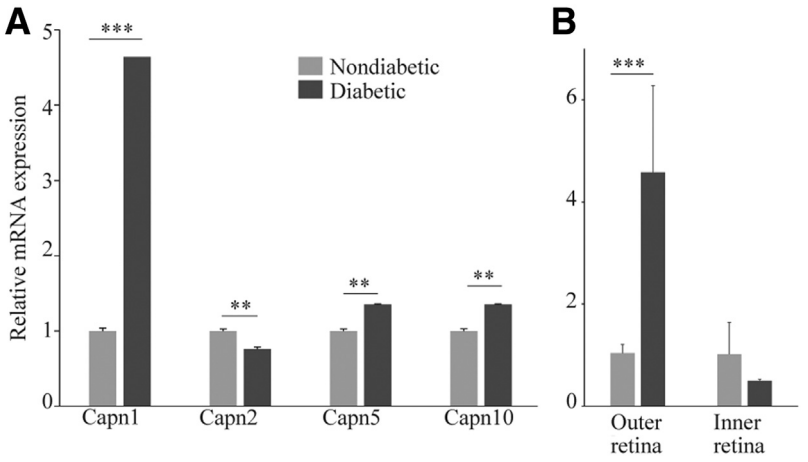

Figure 4 Diabetes induces calpain1 gene expression in photoreceptor cells. **A:** Whole retinas of diabetic and nondiabetic mice were subjected to quantitative RT-PCR (qRT-PCR) to evaluate the expression of different calpain isoforms, calpain1, 2, 5, and 10. The results showed that diabetes induced a fivefold increase of Capn1 in diabetic retinas. **B:** Retina from diabetic and nondiabetic mice were bisected into photoreceptors (outer retina) and inner retina using a vibratome, and then mRNA levels were measured using qRT-PCR. Data are expressed as means ± SD. $n = 3$ measurements, 2 retinas from each mouse were pooled ($n = 3$ to 4). $^{**}P \leq 0.01$, $^{***}P \leq 0.001$ (two-tailed unpaired t-test).

measured after lowering intracellular Ca^{2+} by applying the Ca^{2+} ionophore, ionomycin (10 μmol/L), in a Ca^{2+}-free medium with the chelator EGTA (5 mmol/L). R_{max} was then measured by applying Ames' medium in the continued presence of ionomycin. These data show that resting intracellular Ca^{2+} levels were elevated significantly in the somas of rod cells from diabetic mice ($P = 0.0082$) (Figure 2B).

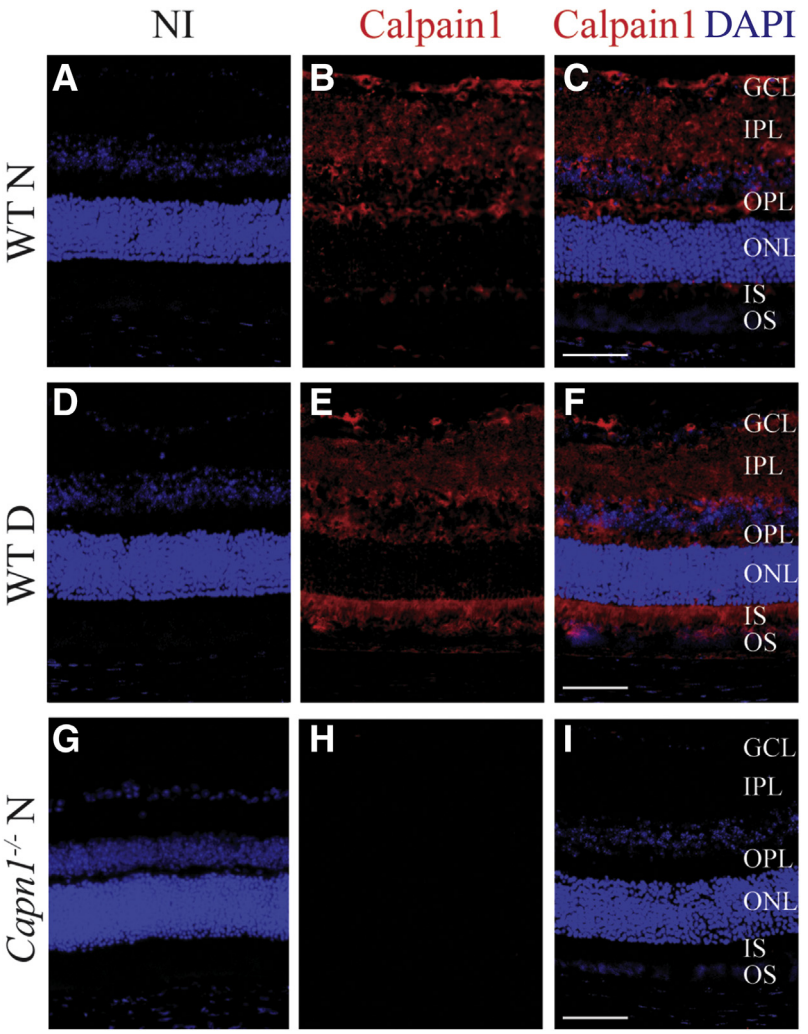

Figure 5 Immunolocalization of calpain1 in the retinas of nondiabetic (N) and 2-month diabetic mice (D). **G—I:** Sections from *Capn1*$^{-/-}$ mice were used as negative control. **A**, **D**, and **G:** Control sections were treated with the serum from nonimmunized animals (NI). **B**, **C**, **E**, **F**, **H**, and **I:** Nuclei were stained with DAPI (in blue), and Capn1 (in red). All images are representative. $n = 3$ mice (approximately 5 months) and 1 retina from each mouse. Scale bars: 100 μm. GCL, ganglion cell layer; IPL, inner plexiform layer; IS, photoreceptors inner segment; ONL, outer nuclear layer; OPL, outer plexiform layer; OS, photoreceptors outer segment; WT, wild type.

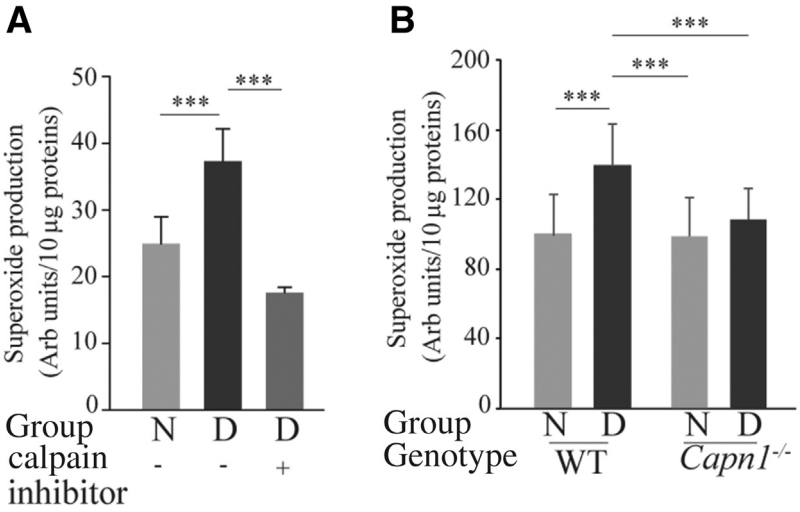

Figure 6 Calpain inhibition (**A**) and deletion (**B**) mitigate diabetes-induced superoxide generation. Calpain inhibitor was administered daily (i.p. injections at a dose of 10 mg/kg). Duration of diabetes was 2 months at the time of this assay, and administration of the inhibitor began promptly after the initiation of diabetes. $n = 4$ to 8 per group. $***P \leq 0.001$. D, diabetic; N, nondiabetic; WT, wild type.

Calpain Activity Is Increased in Photoreceptors of Diabetic Mice

In order to determine whether the diabetes-induced increase in Ca^{2+} in retinal photoreceptor cells was associated with an increase in activity of Ca^{2+}-activated proteases, calpain activity was studied using three different approaches. The first approach was to inject a fluorogenic calpain substrate intravitreally into the eyes of diabetic and nondiabetic mice, letting it incubate in the globe for 2 hours, followed by preparation of cryosections and visualization of sites of activity by fluorescence microscopy. The second method involved incubation of cryosections from freshly frozen eyes with calpain substrate *in vitro*, followed by fluorescence microscopy. In both cases, fluorescence indicating calpain activity was localized mostly to photoreceptor cells in diabetic as compared with nondiabetic mice (Figure 3, A and B). Faint staining of calpain substrate was also present in the outer plexiform layer along with tiny focal deposits of staining in the inner plexiform layer and ganglion cell layer of retinas from diabetic mice. Addition of a CI during incubation with the calpain substrate inhibited the staining in photoreceptor cells, but did not reduce the fluorescence of focal deposits in the inner plexiform layer and ganglion cell layer (Figure 3B), suggesting these were not due to calpain activity. Calpain activation was also assessed by a third method, Western blot using an antibody against the cleaved fragment of spectrin, a molecule of the cytoskeleton and a specific substrate of calpain. This method showed a band at approximately 160 kDa that corresponds to cleaved spectrin in 2-month diabetic mice, which was not seen in nondiabetic controls (Figure 3C).

Increased Expression of Capn1 in Retinas and Freshly Isolated Photoreceptors of Diabetic Mice

Calpain1 (Capn1), 2, 5, and 10 are expressed in the retina.[16,34] Whether diabetes altered their expression in retinas and in photoreceptor cells was investigated in this study. mRNAs of the calpain isoforms evaluated were expressed relatively equally in the whole retina of WT nondiabetic mice. Two months of diabetes led to a fivefold increase in Capn1 and smaller, but significant, increases of 1.3-fold and 1.4-fold for Capn5 and 10 in retinas of diabetic mice, respectively (Figure 4A). By contrast, 2 months of diabetes led to a small, but significant, decrease in the expression of Capn2 (Figure 4A).

Because Capn1 expression was the most dysregulated among the calpains tested in diabetes, and diabetes caused an increase in calpain activity in photoreceptor cells, whether the expression of calpain1 was localized to photoreceptors was next determined. A vibratome was used to divide the fresh retina into a photoreceptor-enriched block (outer retina), and the remaining (inner) retina for comparison. The outer retina from mice diabetic for 2 months had a fivefold increase in the expression of mRNA of Capn1 as compared to that of nondiabetic mice (Figure 4B). By contrast, Capn1 expression was not significantly different in inner retina from diabetic or nondiabetic mice.

Immunofluorescence Detection of *capn1* in the Retinas of 2-Month Diabetic and Nondiabetic Mice

Antibody against calpain1 was used to study the localization of calpain1 isoform within the retina of 2 months diabetic mice and nondiabetic control mice. Retinas from *Capn1*$^{-/-}$ mice were used as a negative control. The retinas of WT nondiabetic mice showed staining in all layers of inner retina; however, in 2-month diabetic retinas, staining was detected in photoreceptor segments in addition to that in the inner retina (Figure 5).

Inhibition or Deletion of *capn1* Inhibit the Diabetes-Induced Increase in Retinal Superoxide

Having demonstrated that diabetes leads to a significant increase of Capn1 expression and activity in photoreceptors,

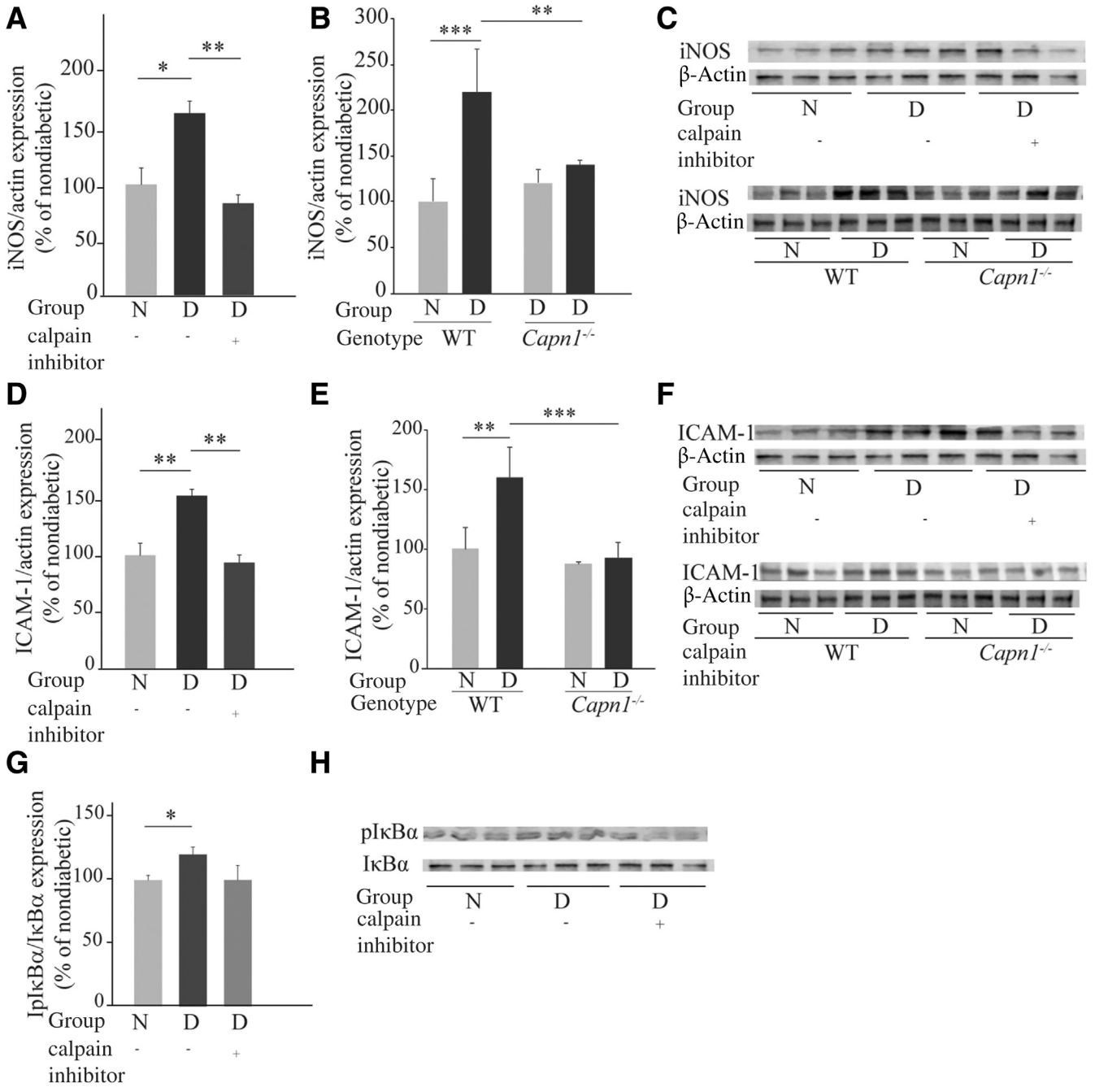

Figure 7 Pharmacologic inhibition of calpain and genetic deletion of *Capn1* mitigate diabetes-induced iNOS, ICAM-1 up-regulation, and pIκBα. **A**, **D**, and **G:** Calpain inhibitor was administered daily to diabetic mice (i.p. daily 10 mg/kg). **B** and **E:** Whole-body deletion of *Capn1*. Duration of diabetes was 2 months at the time of this assay, and administration of the inhibitor began promptly after the initiation of diabetes ($n = 4$ to 7 per group). **C**, **F**, and **H:** Representative immunoblots for iNOS, ICAM-1, β-actin, pIκBα, and IκBα. **A**, **B**, **D**, **E**, and **G:** Summary graph of data for iNOS, ICAM-1, and pIκBα expression determined by image analysis. Data are expressed relative to the expression of β-actin, a housekeeping protein, and IκBα in the. same lanes, for iNOS and ICAM, and for pIκBα, respectively. Data are expressed as a percentage of the value of nondiabetic controls. $^{*}P \leq 0.05$; $^{**}P \leq 0.01$; and $^{***}P \leq 0.001$. D, diabetic; ICAM-1, intercellular adhesion molecule 1; iNOS, inducible nitric oxide synthase; N, nondiabetic.

whether calpain contributed to the diabetes-induced increase in retinal superoxide and inflammation was tested. Diabetic WT mice received a daily injection of CI (MDL 27180, a potent and selective cell-permeable calpain and cathepsin B inhibitor) in dimethyl sulfoxide at a dose of 10 mg/kg body weight for 2 months. Daily administration of the CI significantly suppressed the diabetes-induced increase in retinal superoxide generation (Figure 6A) without affecting glycemia in those animals (Table 1). Similar conclusions were reached in diabetic $Capn1^{-/-}$ mice (Figure 6B) at 2 months of diabetes. Thus, calpain activity, particularly that from calpain1, accounted for the diabetes-induced increase in retinal superoxide.

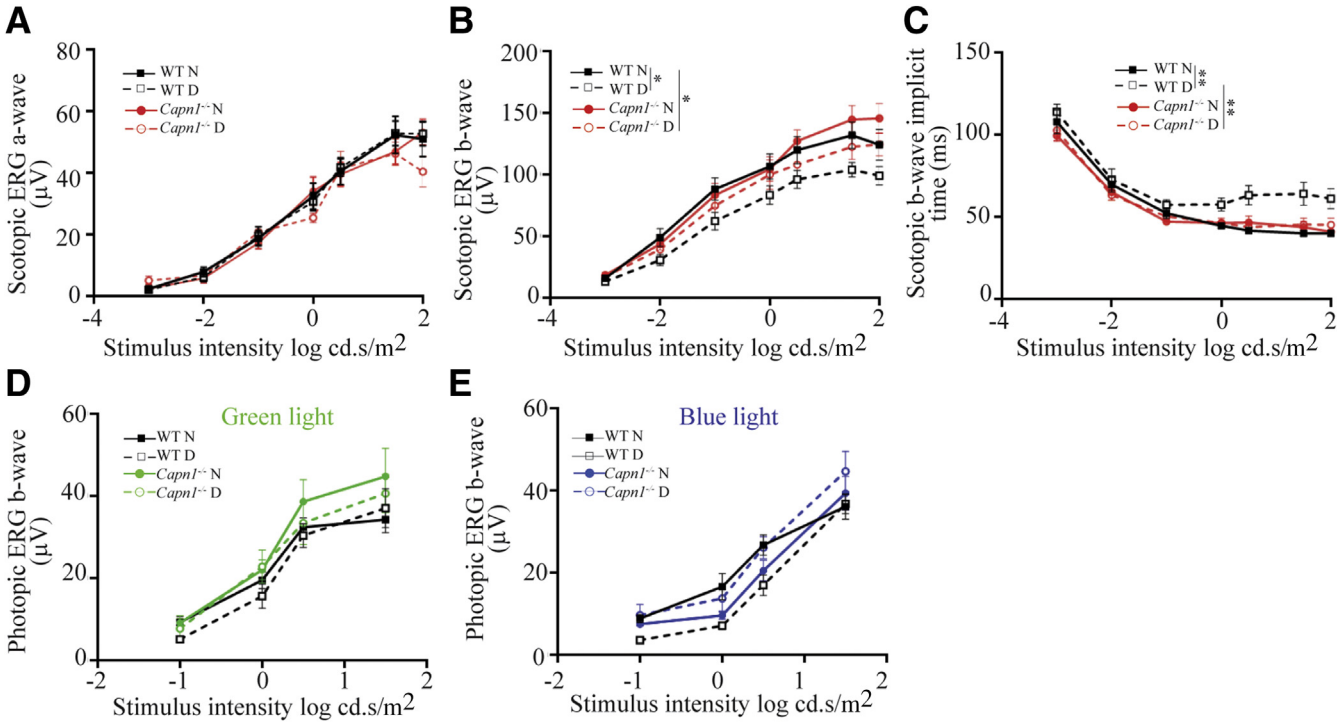

Figure 8 Physiologic testing on the effects of *Capn1* deletion on retinal function. ERG response functions were recorded to evaluate the impact of *Capn1* deletion and diabetes on retinal function under scotopic conditions; both a-wave (**A**), b-wave (**B**), and scotopic b-wave implicit time (**C**), and photopic b-wave for green (**D**) and blue (**E**) light. In WT mice, 2 months of diabetes significantly reduced scotopic b-wave and increased scotopic implicit time when compared with nondiabetic controls; the deletion of *Capn1* significantly inhibited the reduction of scotopic b-wave and the increase of scotopic b-wave implicit time in diabetic $Capn1^{-/-}$ mice. Data are expressed as means ± SEM. $n = 10$ to 14 eyes. $^{*}P \leq 0.05$, $^{**}P \leq 0.01$. D, diabetic; ERG, electroretinographic; N, nondiabetic; WT, wild type.

Inhibition of Calpain and Deletion of *Capn1* Suppress the Diabetes-Induced Increase in Expression of Proinflammatory iNOS and ICAM-1 in the Retina

Having demonstrated that calpain inhibition or deletion of *Capn1* inhibit superoxide generation in the retinas of diabetic mice, the contribution of calpain to the diabetes-induced increase in expression of proinflammatory proteins, iNOS and ICAM-1 was examined next. Diabetes increases the expression of iNOS and ICAM-1.[7,35] Daily administration of CI or deletion of *calpain1* mitigated the diabetes-induced increases in iNOS expression (Figure 7, A–C). Similarly, the expression of ICAM-1 was significantly reduced in diabetic mice treated daily with CI, as well as in diabetic $Capn1^{-/-}$ mice (Figure 7, D–F). Diabetes significantly increased the expression of pIκBα, and daily treatment of diabetic mice with CI decreased that expression, but the decrease did not reach statistical significance (Figure 7, G and H).

Visual Function

To examine overall retinal function, ERGs were recorded under dark- and light-adapted conditions from nondiabetic and diabetic (2-month) $Capn1^{-/-}$ and WT mice. Two months of diabetes significantly reduced scotopic b-wave in WT mice when compared with nondiabetic controls. This decrease was significantly inhibited in diabetic $Capn1^{-/-}$ mice (Figure 8). Likewise, 2 months of diabetes significantly increased the scotopic b-wave implicit time in WT mice, and deletion of *Capn1* significantly mitigated these increases in nondiabetic and diabetic (2-month) $Capn1^{-/-}$ mice (Figure 8).

Diabetes-Induced Up-Regulation of Calpain Affects the Photoreceptor Proteome

Calpain system activation can lead to cleavage, modification, or activation of wide range of target proteins.[36] Hence, diabetes-induced changes in proteins were investigated using proteomic techniques on freshly isolated photoreceptors. A vibratome was used to isolate the photoreceptor-enriched outer retina from the rest of the retina (inner retina). The authors identified 15 proteins in the photoreceptor-enriched outer retina whose expression was either abnormally increased or decreased in diabetes, and in which the diabetes-induced change in expression was inhibited (maintained at near-normal levels) by daily injection of the CI (Table 2).

In an effort to investigate whether any of these proteins accounted for the calpain-induced increase in photoreceptor cells in diabetes, the study focused initially on WWOX, a tumor suppressor that gets activated under stress conditions (including metabolic disorders, immune defects, and

Table 2 Proteomics Data Featuring Proteins That Are Either Increased or Decreased in Diabetic Mouse Photoreceptors, Normalized by the Calpain Inhibitor

Protein ID	Protein names	Gene name	# of peptides	Mean			*P* value	
				N	D	DT	D-N	DT-D
Proteins increased in diabetic and decreased by calpain inhibitor								
O884852; O88485	Cytoplasmic dynein 1	*Dync1*	10	0.27	0.58	0.18	0.03	0.007
Q9CR09	Ubiquitin-fold modifier-conjugating enzyme 1	*Ufc1*	2	−3.92	−3.08	−1.08	0.04	0.02
Q91WL83; Q91WL8-4; Q91WL8; Q91WL8-2	WW domain-containing oxidoreductase	*Wwox*	4	−3.55	−1.75	−2.94	0.002	0.01
P61226; Q80ZJ12; Q8BU31	Ras-related protein Rap-2b; Ras-related protein Rap-2a; Ras-related protein Rap-2c	*Rap2b; Rap2a;Rap2c*	6	1.14	1.55	−0.66	0.02	0.04
O35654	DNA polymerase delta subunit 2	*Pold2*	3	−2.36	−1.98	−3.25	0.02	0.02
Q8BYM5	Neuroligin-3	*Nlgn3*	5	−1.18	−0.43	−1.10	0.02	0.02
Q91YP2	Neurolysin, mitochondrial	*Nln*	4	−3.39	−1.58	−3.26	0.04	0.04
Proteins decreased in diabetic and increased by calpain inhibitor								
E9Q735	Ubiquitination factor E4A	*Ube4a*	8	0.59	0.12	0.79	0.004	0.02
P15208	Insulin receptor; insulin receptor subunit alpha; insulin receptor subunit beta	*Insr*	3	−3.32	−4.02	−2.78	0.03	0.01
P01872; P01872-2	Ig mu chain C region	*Ighm*	2	−3.56	−4.87	−2.40	0.03	0.01
Q925N0	Sideroflexin-5	*Sfxn5*	11	2.25	1.74	2.22	0.05	0.01
P62488	DNA-directed RNA polymerase II subunit RPB7	*Polr2g*	2	−0.20	−0.85	−0.08	0.03	0.01
Q8CCJ42; Q8CCJ4	APC membrane recruitment protein 2	*Amer2*	2	−0.32	−4.03	−0.32	0.001	0.01
Q9QZH6	Evolutionarily conserved signaling intermediate in Toll pathway, mitochondrial	*Ecsit*	2	−3.64	−4.35	−3.13	0.02	0.02
P84099	60S ribosomal protein L19	*Rpl19*	3	1.30	−0.20	1.34	0.03	0.04

D, diabetic; DT, diabetic treated with calpain inhibitor; N, nondiabetic.

neurodegenerative diseases), and acts as a regulator of ROS.[37–39] The expression of Wwox in photoreceptor-enriched outer retina was further confirmed by qRT-PCR. Wwox mRNA in the photoreceptor-enriched outer retina from mice diabetic for 2 months was increased 1.9-fold compared with that in nondiabetic controls (0.965 ± 0.13 versus 1.98 ± 0.21). This was confirmed *in vitro*.

661W cells incubated in 30 mmol/L glucose generated more superoxide than in 5 mmol/L glucose (100 ± 2.4 arbitrary units versus 180 ± 15 with 5 mmol/L and 30 mmol/L, respectively), and gene expression of Wwox was significantly increased in cells incubated in 30 mmol/L glucose compared with cells incubated in 5 mmol/L glucose (1.03 ± 0.3 versus 1.75 ± 0.2), CI significantly inhibited this increase in Wwox expression (1.75 ± 0.2 versus 1.13 ± 0.2) (Figure 9A). In a different set of experiments, 661W cells were incubated with D-mannitol (osmotic control), and superoxide assay was performed. The cells incubated in 30 mmol/L D-mannitol were comparable to control (1428 ± 86 vs. 240 ± 29 arbitrary units/10^6 cells, and cells treated with 30 mmol/L glucose and 30 mmol/L D-mannitol, respectively). Cells treated with siRNA targeting *Wwox* gene inhibited Wwox mRNA by 65% compared with that in cells treated with scrambled siRNA as a control (Figure 9B), and significantly reduced the superoxide production in high glucose by 27% and 37% in the two different concentrations of siRNA (5 and 25 pmol), respectively, compared with scrambled siRNA (Figure 9C).

Discussion

The present study led to the novel findings that diabetes causes an increase in intracellular Ca^{2+} levels and increased calpain activity in photoreceptor cells of diabetic mice, and

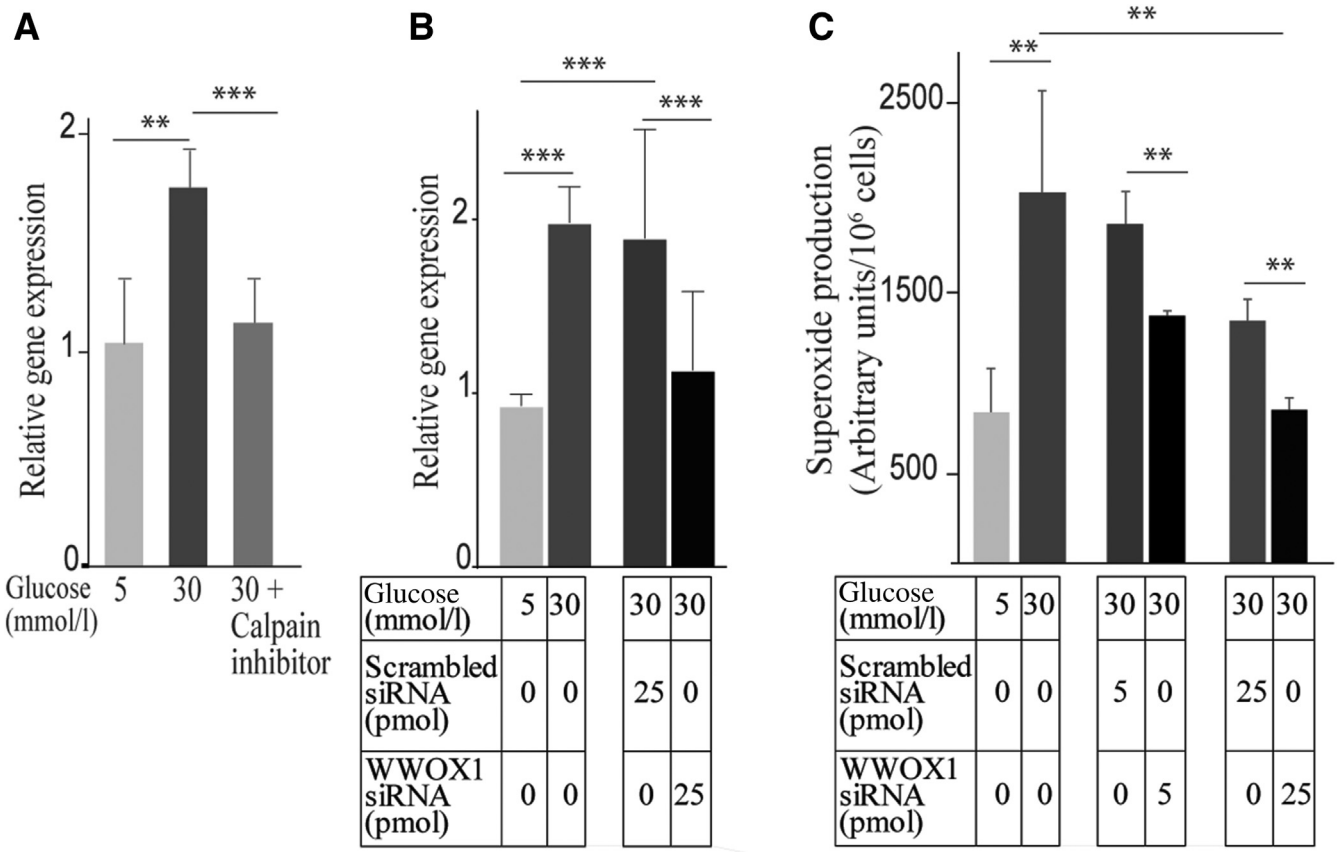

Figure 9 WWOX is involved in superoxide generation by 661W cells incubated in nondiabetic (5 mmol/L) and diabetic (30 mmol/L) glucose. **A:** *Wwox* gene expression was increased twofold in the diabetic-like glucose concentration, and calpain inhibitor inhibited diabetes-induced Wwox expression. 66W1 photoreceptors were incubated in low glucose (5 mmol/L = normal glucose) or high glucose (30 mmol/L = diabetes-like glucose concentration) without or with calpain inhibitor (10 μmol/L). mRNA levels were performed using quantitative RT-PCR. **B** and **C:** *Wwox* knockdown using siRNA inhibited the glucose-induced increase *Wwox* gene expression (**B**) and superoxide generation (**C**) as compared with cells treated with scrambled-siRNA. Data are expressed as means ± SD. $n = 2$ replications of the results . $^{**}P \leq 0.01$, $^{***}P \leq 0.001$.

that the diabetes-induced increase in oxidative stress and expression of proinflammatory proteins in photoreceptor cells can be mitigated by pharmacological inhibition or genetic deletion of *Capn1*. Additionally, calpain activity regulates the gene product Wwox in photoreceptor cells, and mitigation of diabetes-induced increase in Wwox by CI or WWOX siRNA inhibits the increase in photoreceptor cell superoxide caused by high glucose (Figure 10). Taken together, these data form a new picture of how pathogenic oxidative stress and inflammation can develop early in the course of DR, thus highlighting new treatment targets. This study particularly focused on Ca^{2+} and calpain activity dysregulation on photoreceptor cells in the diabetic retina, and more work is needed to understand the effect of Ca^{2+} and calpain activity in other part of the retina.

Experimental studies have identified photoreceptors as a major contributor to the pathogenesis of DR, and the oxidative stress and inflammation that develop in retinas of diabetic animals seem secondary to changes initiated in retinal photoreceptor cells.[2,3,7,40] The use of freshly isolated photoreceptors in *ex vivo* and *in vitro* studies shows that when incubated in elevated glucose, photoreceptors *per se* are an important source of the inflammatory proteins in diabetes.[26,41] These data further support and extend the novel hypothesis that retinal photoreceptor cells are responsible for the pathogenesis of early DR.

Calcium is a ubiquitous intracellular messenger, acting as a regulator of multiple physiological functions. Nevertheless, sustained perturbation in intracellular calcium levels can have deleterious effects, leading to cell dysfunction or cell death. In the present study, a significant twofold increase in intracellular Ca^{2+} was found in rods from dark-adapted diabetic mice compared with those in nondiabetic mice. Increases of twofold or more (such as was found in the photoreceptor cells) in cytosolic calcium in neurons are sufficient to activate downstream signaling pathways and stimulate mitochondrial energy production with increased production of free radicals from mitochondria and/or NADPH oxidase.[7,42–50] The present results are thus in line with the notion that abnormal accumulation of cytosolic Ca^{2+} increases oxidative stress, particularly in photoreceptors, which have a very weak Ca^{2+} buffering capacity[51] and possess at least 75% of total retinal mitochondria.[52] The mechanism by which diabetes increases intracellular Ca^{2+}

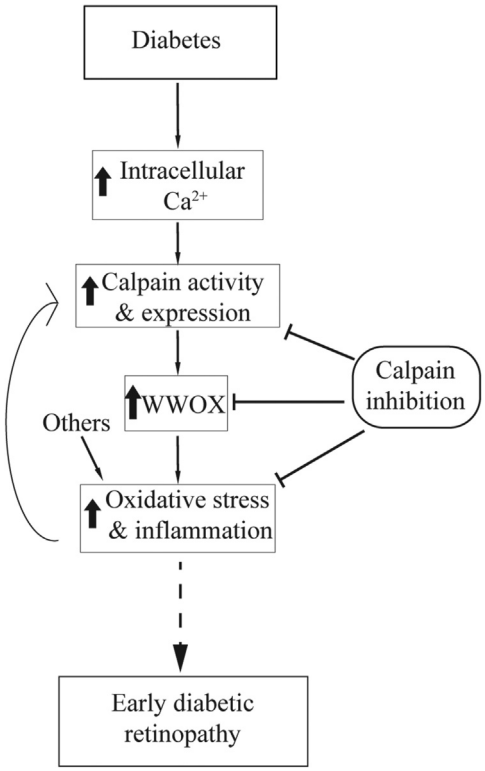

Figure 10 Postulated schematic relationship between dysregulation of intracellular $Ca2^{+}$ and calpain activation in photoreceptor cells, the induction of oxidative stress and inflammation. **Solid lines** show confirmed pathways, and **dotted lines** show the pathway suggested.

in photoreceptor cells is not clear, but unlike most other neurons, photoreceptors do not have conventional synaptic inputs and rely on plasma membrane calcium channels, such as LTCCs, for Ca^{2+} influx.[53–57] Previous studies have demonstrated defects in LTCC function and ion movement into photoreceptor cells of diabetic rodents.[10] In nondiabetic mice, sustained illumination causes rod membrane hyperpolarization, closure of LTCCs, and depletion of endoplasmic reticulum calcium stores.[58] As a result, non-LTCCs open in the plasma membrane and allow extracellular Ca^{2+} entry (ie, store-operated calcium entry).[58,59] In diabetes, a sustained, paradoxical closure of rods LTCCs, but cytosolic Ca^{2+} accumulation occurs in the dark (Figure 2). Diabetes may engage an alternative Ca^{2+} influx pathway involving transient receptor potential channels found in mouse rods[50,56] and impair retinal Ca^{2+} efflux via Ca^{2+} ATPase.[60] Together, these events may lead to excessive cytosolic Ca^{2+} accumulation, but more work is needed to test this proposed signaling pathway.

Increases in intracellular calcium can activate calpains, a family of calcium-dependent nonlysosomal proteases. Calpain1 (μ-calpain) and calpain-2 (m-calpain) are the best characterized and most ubiquitously expressed calpains, and are activated by micromolar and millimolar calcium concentrations, respectively. Calpains belong to a family of calcium-dependent cysteine proteases with at least 16 members and are widely distributed in cells, including immune cells[61] and vascular cells.[62] They can be detected in multiple subcellular organelles, including mitochondria.[63,64] The authors found that the elevated intracellular calcium in photoreceptor cells was associated with a significant increase in the activity and expression of Capn1 in photoreceptor cells. Several studies have shown that the calcium concentration is dysregulated in cardiomyocytes, hepatocytes, and platelets during diabetes,[36,65,66] and this calcium accumulation leads to calpain activation.[18,67–71]

Both oxidative stress and inflammation are implicated in the development of vascular lesions that are characteristic of the early stages of DR.[72–74] Inhibition of oxidative stress or overexpression of antioxidant enzymes can reduce diabetes-induced degeneration of retinal capillaries.[9,75–77] Many of the molecular abnormalities (such as iNOS and ICAM-1) that develop in the retina during diabetes are consistent with inflammation, and inhibiting or deleting them blocks the development of vascular lesions characteristic of the early stages of DR.[77–81] The present study showed that pharmacologic inhibition of the diabetes-induced increase in calpain activity and genetic deletion of *capn1* suppressed the diabetes-induced superoxide generation in the retina. Additionally, calpain activation targets proteins in mitochondria that compromise mitochondrial function, resulting in excessive ROS generation and oxidative stress.[18,82,83]

This study showed that a CI or *capn1* deletion inhibit diabetes-induced increases in the expression of iNOS and ICAM-1 in the retina. Expression of both proteins is regulated by NF-κB, subsequent to degradation of IκBα, and translocation of NF-κB to nucleus. Several studies have shown that IκBα can be degraded in a calpain-dependent manner independent of the ubiquitin-proteasome system.[84,85] However, the mechanism by which calpain1 regulates the diabetes-induced iNOS, ICAM-1, and other proinflammatory proteins requires further study.

Proteomic studies were conducted to identify the substrates of calpain in diabetic photoreceptors that might explain calpain-induced superoxide generation and inflammation. These studies identified several proteins whose expression was altered in diabetes, and whose expression defect was at least partially mitigated by pharmacologic inhibition of calpain. In particular, WWOX, also known as WWOX/WOX1 or FOR,[38] seemed of interest related to diabetes and oxidative stress. WWOX is located ubiquitously within the cells and can be found in the cytoplasm, cell membrane, cytoskeleton, organelles, and nucleus.[38,86,87] This 46-KDa protein interacts with proline-tyrosine motif-containing proteins via its WW1 domain, which regulates its localization and transcriptional function.[86] WWOX becomes activated under stress conditions to act as a regulator of ROS.[37–39] Activated Wwox was found in degenerating photoreceptors in a model of light-induced retinal damage as well as in *rd* mice with an inherited retinal degeneration.[38] O'Keefe et al[39] (2011) reported that the highly conserved *Drosophila* orthologue of WWOX has

biologically significant roles in pathways linked to aerobic metabolism and oxidative stress. Here, the study shows that knockdown of *Wwox* using siRNA significantly inhibited the oxidative stress induced in retinal photoreceptor cells in elevated levels of glucose, and therefore postulate that WWOX contributes to the diabetes-induced oxidative stress that develops in retinal cells and perhaps other tissues.

How WWOX might affect ROS generation in diabetic retina is not yet clear. However, WWOX is implicated in regulation of the canonical and noncanonical NF-κB pathways.[87,88] Wwox physically binds to IκBα, the inhibitor of NF-κB, thereby stimulating NF-κB−induced promoter activation.[87] In addition, Wwox interacts with the hypoxia-inducible transcription factor, a master oxygen sensor and master transcriptional regulator of a variety of processes including energy metabolism.[40,89]

In summary, diabetes results in calcium accumulation in rod photoreceptors, and this increase is associated with increased calpain activity and expression of Capn1 in photoreceptors. Calpain inhibition or deletion abrogating the diabetes-induced superoxide generation and induction of iNOS and ICAM-1 indicates that calpains play an important role in diabetes-induced oxidative stress and inflammation that occurs in the retina. Wwox was identified as a substrate for calpain, and the authors postulate that one step between calpain activation and the development of retinal oxidative stress and inflammation in diabetes involves WWOX. Inhibiting calcium accumulation, calpain activation, and/or WWOX up-regulation in diabetes merit further study as potential therapeutic targets to mitigate the pathogenesis of early stages of DR.

Acknowledgments

We acknowledge the services of the CWRU Visual Science Research Center Core Facilities for mouse breeding (Heather Butler and Kathryn Franke), animal genotyping (John Denker), tissue sectioning (Catherine Doller), and microscopy (Anthony Gardella). We thank Dr. Athar Chishti (Tufts University School of Medicine, Boston, MA) for providing *Capn*$^{-/-}$ mice, Dr. Avery Sears for help with intravitreal injections, and Dr. Henri Leinonen for discussion about ERG data analysis. Dr. Belinda Willard from the Proteomics laboratory at the Cleveland Clinic Foundation conducted proteomic studies.

References

1. Arden GB: The absence of diabetic retinopathy in patients with retinitis pigmentosa: implications for pathophysiology and possible treatment. Br J Ophthalmol 2001, 85:366−370
2. Berkowitz BA: Preventing diabetic retinopathy by mitigating subretinal space oxidative stress in vivo. Vis Neurosci 2020, 37:E002
3. Kern TS, Berkowitz BA: Photoreceptors in diabetic retinopathy. J Diabetes Investig 2015, 6:371−380
4. Berkowitz BA, Bissig D, Patel P, Bhatia A, Roberts R: Acute systemic 11-cis-retinal intervention improves abnormal outer retinal ion channel closure in diabetic mice. Mol Vis 2012, 18:372−376
5. Berkowitz BA, Gradianu M, Schafer S, Jin Y, Porchia A, Iezzi R, Roberts R: Ionic dysregulatory phenotyping of pathologic retinal thinning with manganese-enhanced MRI. Invest Ophthalmol Vis Sci 2008, 49:3178−3184
6. Berkowitz BA, Grady EM, Khetarpal N, Patel A, Roberts R: Oxidative stress and light-evoked responses of the posterior segment in a mouse model of diabetic retinopathy. Invest Ophthalmol Vis Sci 2015, 56:606−615
7. Du Y, Veenstra A, Palczewski K, Kern TS: Photoreceptor cells are major contributors to diabetes-induced oxidative stress and local inflammation in the retina. Proc Natl Acad Sci U S A 2013, 110:16586−16591
8. Krizaj D, Copenhagen DR: Calcium regulation in photoreceptors. Front Biosci 2002, 7:d2023−d2044
9. Berkowitz BA, Gradianu M, Bissig D, Kern TS, Roberts R: Retinal ion regulation in a mouse model of diabetic retinopathy: natural history and the effect of Cu/Zn superoxide dismutase overexpression. Invest Ophthalmol Vis Sci 2009, 50:2351−2358
10. Berkowitz BA, Roberts R, Stemmler A, Luan H, Gradianu M: Impaired apparent ion demand in experimental diabetic retinopathy: correction by lipoic acid. Invest Ophthalmol Vis Sci 2007, 48:4753−4758
11. Gillardon F, Zimmermann M, Uhlmann E: Expression of c-Fos and c-Jun in the cornea, lens, and retina after ultraviolet irradiation of the rat eye and effects of topical antisense oligodeoxynucleotides. Br J Ophthalmol 1995, 79:277−281
12. Azuma M, Shearer TR: The role of calcium-activated protease calpain in experimental retinal pathology. Surv Ophthalmol 2008, 53:150−163
13. Frustaci A, Kajstura J, Chimenti C, Jakoniuk I, Leri A, Maseri A, Nadal-Ginard B, Anversa P: Myocardial cell death in human diabetes. Circ Res 2000, 87:1123−1132
14. Hirata M, Shearer T, Azuma M: Hypoxia activates calpains in the nerve fiber layer of monkey retinal explants. Invest Ophthalmol Vis Sci 2015, 56:6049−6057
15. Joyal J-S, Sun Y, Gantner ML, Shao Z, Evans LP, Saba N, Fredrick T, Burnim S, Kim JS, Patel G, Juan AM, Hurst CG, Hatton CJ, Cui Z, Pierce KA, Bherer P, Aguilar E, Powner MB, Vevis K, Boisvert M, Fu Z, Levy E, Fruttiger M, Packard A, Rezende FA, Maranda B, Sapieha P, Chen J, Friedlander M, Clish CB, Smith LEH: Retinal lipid and glucose metabolism dictates angiogenesis through the lipid sensor Ffar1. Nat Med 2016, 22:439−445
16. Paquet-Durand F, Azadi S, Hauck SM, Ueffing M, van Veen T, Ekström P: Calpain is activated in degenerating photoreceptors in the rd1 mouse. J Neurochem 2006, 96:802−814
17. Vanderklish PW, Bahr BA: The pathogenic activation of calpain: a marker and mediator of cellular toxicity and disease states. Int J Exp Pathol 2000, 81:323−339
18. Ni R, Zheng D, Xiong S, Hill DJ, Sun T, Gardiner RB, Fan GC, Lu Y, Abel ED, Greer PA, Peng T: Mitochondrial calpain-1 disrupts ATP synthase and induces superoxide generation in type 1 diabetic hearts: a novel mechanism contributing to diabetic cardiomyopathy. Diabetes 2016, 65:255−268
19. Committee for the Update of the Guide for the Care and Use of Laboratory AnimalsNational Research Council: Guide for the Care and Use of Laboratory Animals: Eighth Edition. Washington, DC: National Academies Press, 2011
20. Association for Research in Vision and Ophthalmology: Statement for the Use of Animals in Ophthalmic and Vision Research. Rockville, MD: ARVO, 2016
21. Azam M, Andrabi SS, Sahr KE, Kamath L, Kuliopulos A, Chishti AH: Disruption of the mouse mu-calpain gene reveals an essential role in platelet function. Mol Cell Biol 2001, 21:2213−2220
22. Liu H, Tang J, Du Y, Saadane A, Samuels I, Veenstra A, Kiser JZ, Palczewski K, Kern TS: Transducin1, phototransduction and the

development of early diabetic retinopathy. Invest Ophthalmol Vis Sci 2019, 60:1538−1546
23. Orban T, Leinonen H, Getter T, Dong Z, Sun W, Gao S, Veenstra A, Heidari-Torkabadi H, Kern TS, Kiser PD, Palczewski K: A combination of G protein-coupled receptor modulators protects photoreceptors from degeneration. J Pharmacol Exp Ther 2018, 364: 207−220
24. Saadane A, Mast N, Charvet CD, Omarova S, Zheng W, Huang SS, Kern TS, Peachey NS, Pikuleva IA: Retinal and nonocular abnormalities in Cyp27a1(-/-)Cyp46a1(-/-) mice with dysfunctional metabolism of cholesterol. Am J Pathol 2014, 184:2403−2419
25. Du Y, Miller CM, Kern TS: Hyperglycemia increases mitochondrial superoxide in retina and retinal cells. Free Radic Biol Med 2003, 35: 1491−1499
26. Tonade D, Liu H, Kern TS: Photoreceptor cells produce inflammatory mediators that contribute to endothelial cell death in diabetes. Invest Ophthalmol Vis Sci 2016, 57:4264−4271
27. Tang J, Du Y, Lee CA, Talahalli R, Eells JT, Kern TS: Low-intensity far-red light inhibits early lesions that contribute to diabetic retinopathy: in vivo and in vitro. Invest Ophthalmol Vis Sci 2013, 54: 3681−3690
28. Cui W, Taub DD, Gardner K: qPrimerDepot: a primer database for quantitative real time PCR. Nucleic Acids Res 2007, 35:D805−D809
29. Du Y, Cramer M, Lee CA, Tang J, Muthusamy A, Antonetti DA, Jin H, Palczewski K, Kern TS: Adrenergic and serotonin receptors affect retinal superoxide generation in diabetic mice: relationship to capillary degeneration and permeability. FASEB J 2015, 29: 2194−2204
30. Shevchenko A, Tomas H, Havlis J, Olsen JV, Mann M: In-gel digestion for mass spectrometric characterization of proteins and proteomes. Nat Protoc 2006, 1:2856−2860
31. Cox J, Mann M: MaxQuant enables high peptide identification rates, individualized p.p.b.-range mass accuracies and proteome-wide protein quantification. Nat Biotechnol 2008, 26:1367−1372
32. Cox J, Neuhauser N, Michalski A, Scheltema RA, Olsen JV, Mann M: Andromeda: a peptide search engine integrated into the MaxQuant environment. J Proteome Res 2011, 10: 1794−1805
33. Tyanova S, Temu T, Sinitcyn P, Carlson A, Hein MY, Geiger T, Mann M, Cox J: The Perseus computational platform for comprehensive analysis of (prote)omics data. Nat Methods 2016, 13: 731−740
34. Azuma M, Sakamoto-Mizutani K, Nakajima T, Kanaami-Daibo S, Tamada Y, Shearer TR: Involvement of calpain isoforms in retinal degeneration in WBN/Kob rats. Comp Med 2004, 54:533−542
35. Liu H, Tang J, Du Y, Saadane A, Tonade D, Samuels I, Veenstra A, Palczewski K, Kern TS: Photoreceptor cells influence retinal vascular degeneration in mouse models of retinal degeneration and diabetes. Invest Ophthalmol Vis Sci 2016, 57:4272−4281
36. Randriamboavonjy V, Isaak J, Elgheznawy A, Pistrosch F, Frömel T, Yin X, Badenhoop K, Heide H, Mayr M, Fleming I: Calpain inhibition stabilizes the platelet proteome and reactivity in diabetes. Blood 2012, 120:415−423
37. Chang H-T, Liu C-C, Chen S-T, Yap YV, Chang N-S, Sze C-I: WW domain-containing oxidoreductase in neuronal injury and neurological diseases. Oncotarget 2014, 5:11792−11799
38. Chen S-T, Chuang J-I, Cheng C-L, Hsu L-J, Chang N-S: Light-induced retinal damage involves tyrosine 33 phosphorylation, mitochondrial and nuclear translocation of WW domain-containing oxidoreductase in vivo. Neuroscience 2005, 130:397−407
39. O'Keefe LV, Colella A, Dayan S, Chen Q, Choo A, Jacob R, Price G, Venter D, Richards RI: Drosophila orthologue of WWOX, the chromosomal fragile site FRA16D tumour suppressor gene, functions in aerobic metabolism and regulates reactive oxygen species. Hum Mol Genet 2011, 20:497−509
40. Kern TS: Do photoreceptor cells cause the development of retinal vascular disease? Vis Res 2017, 139:65−71
41. Tonade D, Liu H, Palczewski K, Kern TS: Photoreceptor cells produce inflammatory products that contribute to retinal vascular permeability in a mouse model of diabetes. Diabetologia 2017, 60: 2111−2120
42. Bréchard S, Tschirhart E: Regulation of superoxide production in neutrophils: role of calcium influx. J Leukoc Biol 2008, 84: 1223−1237
43. Ermak G, Davies KJ: Calcium and oxidative stress: from cell signaling to cell death. Mol Immunol 2002, 38:713−721
44. Guzman JN, Sanchez-Padilla J, Wokosin D, Kondapalli J, Ilijic E, Schumacker PT, Surmeier DJ: Oxidant stress evoked by pacemaking in dopaminergic neurons is attenuated by DJ-1. Nature 2010, 468: 696−700
45. Kowluru RA, Kowluru A, Veluthakal R, Mohammad G, Syed I, Santos JM, Mishra M: TIAM1-RAC1 signalling axis-mediated activation of NADPH oxidase-2 initiates mitochondrial damage in the development of diabetic retinopathy. Diabetologia 2014, 57:1047−1056
46. Rojas M, Zhang W, Xu Z, Lemtalsi T, Chandler P, Toque HA, Caldwell RW, Caldwell RB: Requirement of NOX2 expression in both retina and bone marrow for diabetes-induced retinal vascular injury. PLoS One 2013, 8:e84357
47. Sharma AK, Rohrer B: Sustained elevation of intracellular cGMP causes oxidative stress triggering calpain-mediated apoptosis in photoreceptor degeneration. Curr Eye Res 2007, 32:259−269
48. Szabo ME, Haines D, Garay E, Chiavaroli C, Farine JC, Hannaert P, Berta A, Garay RP: Antioxidant properties of calcium dobesilate in ischemic/reperfused diabetic rat retina. Eur J Pharmacol 2001, 428: 277−286
49. Verkhratsky A, Fernyhough P: Mitochondrial malfunction and Ca2+ dyshomeostasis drive neuronal pathology in diabetes. Cell Calcium 2008, 44:112−122
50. Zherebitskaya E, Schapansky J, Akude E, Smith DR, Van der Ploeg R, Solovyova N, Verkhratsky A, Fernyhough P: Sensory neurons derived from diabetic rats have diminished internal Ca2+ stores linked to impaired re-uptake by the endoplasmic reticulum. ASN Neuro 2012, 4:e00072
51. Van Hook MJ, Thoreson WB: Endogenous calcium buffering at photoreceptor synaptic terminals in salamander retina. Synapse 2014, 68:518−528
52. Johnson JE Jr, Perkins GA, Giddabasappa A, Chaney S, Xiao W, White AD, Brown JM, Waggoner J, Ellisman MH, Fox DA: Spatiotemporal regulation of ATP and Ca2+ dynamics in vertebrate rod and cone ribbon synapses. Mol Vis 2007, 13:887−919
53. Baumann L, Gerstner A, Zong X, Biel M, Wahl-Schott C: Functional characterization of the L-type Ca2+ channel Cav1.4alpha1 from mouse retina. Invest Ophthalmol Vis Sci 2004, 45:708−713
54. Busquet P, Nguyen NK, Schmid E, Tanimoto N, Seeliger MW, Ben-Yosef T, Mizuno F, Akopian A, Striessnig J, Singewald N: CaV1.3 L-type Ca2+ channels modulate depression-like behaviour in mice independent of deaf phenotype. Int J Neuropsychopharmacol 2010, 13:499−513
55. Koschak A, Reimer D, Walter D, Hoda JC, Heinzle T, Grabner M, Striessnig J: Cav1.4alpha1 subunits can form slowly inactivating dihydropyridine-sensitive L-type Ca2+ channels lacking Ca2+-dependent inactivation. J Neurosci 2003, 23:6041−6049
56. Morgans CW, Gaughwin P, Maleszka R: Expression of the alpha1F calcium channel subunit by photoreceptors in the rat retina. Mol Vis 2001, 7:202−209
57. Xiao H, Chen X, Steele EC: Abundant L-type calcium channel Ca(v)1.3 (alpha1D) subunit mRNA is detected in rod photoreceptors of the mouse retina via in situ hybridization. Mol Vis 2007, 13: 764−771
58. Molnar T, Barabas P, Birnbaumer L, Punzo C, Kefalov V, Krizaj D: Store-operated channels regulate intracellular calcium in mammalian rods. J Physiol 2012, 590:3465−3481
59. Fain GL: Why photoreceptors die (and why they don't). Bioessays 2006, 28:344−354

60. Sheikh AQ, Hurley JR, Huang W, Taghian T, Kogan A, Cho H, Wang Y, Narmoneva DA: Diabetes alters intracellular calcium transients in cardiac endothelial cells. PLoS One 2012, 7(5): e36840
61. Mikosik A, Jasiulewics A, Daca A, Henc I, Frąckowiak JE, Ruckemann-Dziurdzińska K, Foerster J, Le Page A, Bryl E, Fulop T, Witkowski JM: Roles of calpain-calpastatin system (CCS) in human T cell activation. Oncotarget 2016, 7:76479−76495
62. Miyazaki T, Taketomi Y, Saito Y, Hosono T, Lei XF, Kim-Kaneyama JR, Arata S, Takahashi H, Murakami M, Miyazaki A: Calpastatin counteracts pathological angiogenesis by inhibiting suppressor of cytokine signaling 3 degradation in vascular endothelial cells. Circ Res 2015, 116:1170−1181
63. Goll DE, Thompson VF, Li H, Wei W, Cong J: The calpain system. Physiol Rev 2003, 83:731−801
64. Kar P, Samant K, Shaikh S, Chowdhury A, Chakraborti T, Chakraborti S: Mitochondrial calpain system: an overview. Arch Biochem Biophys 2010, 495:1−7
65. Studer RK, Ganas L: Effect of diabetes on hormone-stimulated and basal hepatocyte calcium metabolism. Endocrinology 1989, 125: 2421−2433
66. Tschöpe A, Rösen P, Gries FA: Increase in the cytosolic concentration of calcium in platelets of diabetics type II. Thromb Res 1991, 62: 421−428
67. Etwebi Z, Landesberg G, Preston K, Eguchi S, Scalia R: Mechanistic role of the calcium-dependent protease calpain in the endothelial dysfunction induced by MPO (myeloperoxidase). Hypertension 2018, 71:761−770
68. Thompson J, Hu Y, Lesnefsky EJ, Chen Q: Activation of mitochondrial calpain and increased cardiac injury: beyond AIF release. Am J Physiol Heart Circ Physiol 2016, 310:H376−H384
69. Li Y, Li Y, Feng Q, Arnold M, Peng T: Calpain activation contributes to hyperglycaemia-induced apoptosis in cardiomyocytes. Cardiovasc Res 2009, 84:100−110
70. Scalia R, Gong Y, Berzins B, Zhao LJ, Sharma K: Hyperglycemia is a major determinant of albumin permeability in diabetic microcirculation: the role of mu-calpain. Diabetes 2007, 56: 1842−1849
71. Stalker TJ, Gong Y, Scalia R: The calcium-dependent protease calpain causes endothelial dysfunction in type 2 diabetes. Diabetes 2005, 54:1132−1140
72. Brucklacher RM, Patel KM, VanGuilder HD, Bixler GV, Barber AJ, Antonetti DA, Lin C-M, LaNoue KF, Gardner TW, Bronson SK, Freeman WM: Whole genome assessment of the retinal response to diabetes reveals a progressive neurovascular inflammatory response. BMC Med Genomics 2008, 1:26
73. Kern TS: Contributions of inflammatory processes to the development of the early stages of diabetic retinopathy. Exp Diabetes Res 2007, 2007:95103
74. Tang J, Kern TS: Inflammation in diabetic retinopathy. Prog Retin Eye Res 2011, 30:343−358
75. Kanwar M, Chan PS, Kern TS, Kowluru RA: Oxidative damage in the retinal mitochondria of diabetic mice: possible protection by superoxide dismutase. Invest Ophthalmol Vis Sci 2007, 48:3805−3811
76. Kowluru RA: Diabetes-induced elevations in retinal oxidative stress, protein kinase C and nitric oxide are interrelated. Acta Diabetol 2001, 38:179−185
77. Zheng L, Du Y, Miller C, Gubitosi-Klug RA, Ball S, Berkowitz BA, Kern TS: Critical role of inducible nitric oxide synthase in degeneration of retinal capillaries in mice with streptozotocin-induced diabetes. Diabetologia 2007, 50:1987−1996
78. Du Y, Smith MA, Miller CM, Kern TS: Diabetes-induced nitrative stress in the retina, and correction by aminoguanidine. J Neurochem 2002, 80:771−779
79. Joussen AM, Poulaki V, Mitsiades N, Kirchhof B, Koizumi K, Dohmen S, Adamis AP: Nonsteroidal anti-inflammatory drugs prevent early diabetic retinopathy via TNF-alpha suppression. FASEB J 2002, 16:438−440
80. Leal EC, Manivannan A, Hosoya K, Terasaki T, Cunha-Vaz J, Ambrosio AF, Forrester JV: Inducible nitric oxide synthase isoform is a key mediator of leukostasis and blood-retinal barrier breakdown in diabetic retinopathy. Invest Ophthalmol Vis Sci 2007, 48:5257−5265
81. Zheng L, Kern T: Role of nitric oxide, superoxide, peroxynitrite and poly(ADP-ribose) polymerase in diabetic retinopathy. Front Biosci 2009, 14:3974−3987
82. Brulé C, Dargelos E, Diallo R, Listrat A, Béchet D, Cottin P, Poussard S: Proteomic study of calpain interacting proteins during skeletal muscle aging. Biochimie 2015, 92:1923−1933
83. Potz BA, Sabe AA, Elmadhun NY, Sabe SA, Braun BJV, Clements RT, Usheva A, Sellke FW: Calpain inhibition decreases inflammatory protein expression in vessel walls in a model of chronic myocardial ischemia. Surgery 2017, 161:1394−1404
84. Shen J, Channavajhala P, Seldin DC, Sonenshein GE: Phosphorylation by the protein kinase CK2 promotes calpain-mediated degradation of IkappaBalpha. J Immunol 2001, 167:4919−4925
85. Shumway SD, Maki M, Miyamoto S: The PEST domain of IkappaBalpha is necessary and sufficient for in vitro degradation by mu-calpain. J Biol Chem 1999, 274:30874−30881
86. Abu-Odeh M, Bar-Mag T, Huang H, Kim T, Salah Z, Abdeen SK, Sudol M, Reichmann D, Sidhu S, Kim PM, Aqeilan RI: Characterizing WW domain interactions of tumor suppressor WWOX reveals its association with multiprotein networks. J Biol Chem 2014, 289:8865−8880
87. Li M-Y, Lai F-J, Hsu L-J, Lo C-P, Cheng C-L, Lin S-R, Lee M-H, Chang J-Y, Subhan D, Tsai M-S, Sze C-I, Pugazhenthi S, Chang N-S, Chen S-T: Dramatic co-activation of WWOX/WOX1 with CREB and NF-kappaB in delayed loss of small dorsal root ganglion neurons upon sciatic nerve transection in rats. PLoS One 2009, 4:e7820
88. Chen S-J, Huang S-S, Chang N-S: Role of WWOX and NF-κB in lung cancer progression. Transl Respir Med 2013, 1:15
89. Abu-Remaileh M, Aqeilan RI: Tumor suppressor WWOX regulates glucose metabolism via HIF1α modulation. Cell Death Differ 2014, 21:1805−1814